Original Research

Maternal cardiac messenger RNA expression of extracellular matrix proteins in mice during pregnancy and the postpartum period

Megan E Parrott[1], Esam Aljrbi[1], Diane L Biederman[1], Ryan N Montalvo[1], Jeremy L Barth[2] and Holly A LaVoie[1]

[1]Department of Cell Biology and Anatomy, University of South Carolina School of Medicine, Columbia, SC 29208, USA; [2]MUSC Proteogenomics Facility, Department of Regenerative Medicine and Cell Biology, Medical University of South Carolina, Charleston, SC 29425, USA

Corresponding author: Holly A LaVoie. Email: holly.lavoie@uscmed.sc.edu

Impact statement

This study provides the first comprehensive analysis of extracellular matrix protein (ECM) gene expression combined with echocardiographic analyses of heart functional parameters in the murine heart during pregnancy and the early postpartum period. Our findings show regulation of all *Timp*, selected *Mmps*, and *Col1a1*, *Col3a1*, and *Col8a1* mRNA levels with reproductive status, with the greatest number of significant changes occurring in the early postpartum period. Left ventricle cardiac diastolic parameters were the first to change during pregnancy and remained elevated postpartum, whereas systolic parameters were increased in late pregnancy and began to recover during the first week postpartum. These novel findings indicate that although some ECM genes are elevated during late pregnancy, that the postpartum period is a time of robust altered ECM gene expression. These studies provide a basis for examining ECM proteins and their activities in the normal pregnant and postpartum heart and in models of postpartum cardiomyopathy.

Abstract

Pregnancy creates a condition of cardiac volume overload which leads to physiological eccentric hypertrophy of the heart that is reversed in the postpartum period. Pathological cardiac changes in non-pregnant animals are associated with extracellular matrix remodeling. Based on preliminary microarray findings in the hearts of non-pregnant, pregnant, and postpartum mice, we hypothesized that changes in the expression of extracellular matrix protein genes would accompany functional changes in the heart that occur with reproductive status. Adult left ventricle parameters were evaluated by echocardiography in C57BL/6 mice at diestrous (virgin), and at pregnancy days (eds) 10, 12, and 18/19, and at postpartum days (ppds) 1.5 and 7. Twenty-one left ventricle mRNAs were evaluated including genes for tissue inhibitor of metalloproteinases (Timps), several matrix metallopeptidases (Mmps), collagens (Cols), proteoglycans, and enzymes involved in matrix remodeling at similar days except ed10. Compared to virgin mice, left ventricle internal diameter during diastole and end diastolic volumes significantly increased at ed12, ed18/19, ppd1.5, and ppd7. Left ventricle internal diameter during systole was increased at ed18/19 and ppd1.5, and end systolic volume was increased at ed18/19 compared to virgin mice. *Timp1* mRNA levels were higher in late pregnancy and the early postpartum period, and *Timp2-4* mRNAs levels were lower at one or both postpartum days compared to specific earlier time points. *Mmp3* mRNA levels were higher during late pregnancy and postpartum than earlier in pregnancy. *Mmp13* mRNA level was lower at ppd1.5 than late pregnancy, and *Mmp15* mRNA level was lowest at ppd7 compared to all other time points. *Col1a1* and *Col3a1* increased with pregnancy and stayed elevated through ppd7. *Col8a1* mRNA was increased on both postpartum days compared to late pregnancy. Our results indicate that late pregnancy and the first week of the postpartum period are an active time for altered expression of extracellular matrix protein genes.

Keywords: Pregnancy, echocardiography, extracellular matrix, cardiac, gene expression

***Experimental Biology and Medicine* 2018; 243: 1220–1232. DOI: 10.1177/1535370218818457**

Introduction

During pregnancy, the cardiovascular system undergoes significant changes in order to maintain sufficient perfusion of maternal tissue, placenta, and fetal tissue. Intravascular volume can increase by 30–50% during pregnancy.[1,2] With the increased venous return and sustained elevated cardiac volume of pregnancy, the left ventricle (LV) mass increases

with a proportional augmentation of ventricular chamber size and wall thickness.[3,4] This type of eccentric hypertrophy is physiological, meaning it is reversible and typically returns to baseline in humans within a few months to a year of parturition.[5] In mice, studies report that cardiac parameters return to baseline within a few days or even up to a month after delivery.[5–7] Postpartum or peripartum cardiomyopathy is a pathological condition that occurs in late pregnancy, during delivery or within five months of delivery where the heart fails to remodel to the non-pregnant phenotype and remains dilated; this pathological condition can progress to heart failure. As postpartum cardiomyopathy is associated with the physiological changes of pregnancy, understanding the normal heart alterations that occur during pregnancy and its postpartum remodeling period will provide specific targets for further evaluation of the pathological condition.

While the changes in mRNA and protein expression and activity have been widely investigated in pathological hypertrophy states not associated with pregnancy, analyses of such aspects in physiological hypertrophy secondary to pregnancy have been less studied.[7,8] So far, hypertrophy secondary to pregnancy shows no significant changes in the fetal program genes α-myosin heavy chain (α-MHC), β-MHC, atrial natriuretic peptide, phospholamban, and sarcoplasmic reticulum Ca^{2+}-ATPase that are activated in pathological forms of hypertrophy.[8] A study of cardiac electrical properties during pregnancy by Eghbali et al.[9] revealed that Kv4.3 potassium channel mRNA and protein were significantly downregulated in pregnant mice. This is thought to explain the increased QT interval as well as prolonged action potentials observed during pregnancy. Jankowski et al.[10] demonstrated that cardiac endothelial nitric oxide synthase (eNOS) protein abundance and brain natriuretic peptide (BNP) mRNA were downregulated during pregnancy in rats. eNOS is known to be cardioprotective, as is BNP. BNP is produced by the cardiac ventricles in response to pathologic hypertrophy and heart failure.[10] Nitric oxide synthase was found to be more active throughout pregnancy and is linked to the changes in smooth muscle.[11] Previous studies of pregnancy-induced cardiac hypertrophy have identified changes in fibroblast growth factor (FGF)-21, CCAAT/enhancer binding protein-β, and calcineurin.[12–14] Other mediators found to influence cardiac hypertrophy during pregnancy include the mitogen-activated kinase pathway, the phosphatidylinositol-3-kinase/Akt pathway, proteasomal activity, reactive oxygen species, placental growth factor, and Mas receptors.[7,15–18]

Our preliminary goal was to elucidate additional pathways that are altered during pregnancy and the postpartum period in LV to better understand cardiac remodeling that occurs during these physiological states. To this end, we performed a pilot microarray study of wildtype mouse LV during the non-pregnant state, mid and late pregnancy, and the early postpartum period to detect differentially expressed genes. In addition, we evaluated an existing similar dataset from the Gene Expression Omnibus (GEO) database.[7] Both microarray datasets were analyzed for significantly represented gene pathways, and genes encoding ECMs were highly represented. Extracellular matrix molecules including specific collagens, matrix metalloproteinases (Mmps), tissue inhibitor of matrix metalloproteases (Timps) and related proteins are affected in numerous heart pathologies.[19] Given the relevance of this pathway to heart remodeling and that no comprehensive evaluation of ECM gene profiles exists for the heart during pregnancy, the purpose of this current study was to further evaluate possible ECM mRNA expression changes throughout pregnancy and the postpartum period. These gene expression studies were paired with echocardiographic analyses of heart parameters to determine if patterns of cardiac structural change and mRNA expression were coordinated.

Materials and methods

Animals

The animal protocol was approved by the University of South Carolina Institutional Animal Care and Use Committee and all university guidelines were followed for animal use. Animals were housed under standard conditions. Twenty-two approximately three-month-old age-matched timed-pregnant and non-pregnant virgin C57BL/6 mice were obtained from Jackson Laboratories (Bar Harbor, ME). For timed-pregnant echocardiogram studies, 12 additional six to seven-week-old animals were obtained from Jackson Laboratories and allowed to acclimate to their environment for two weeks. The estrous cycles of these later mice and all virgin mice were tracked by performing vaginal lavage as described by Goldman et al.[20] for at least two consecutive cycles to determine when animals were in diestrus. Following initial echocardiograms of animals in diestrous, 12 virgin females were placed in pairs with single males for mating. Mating was confirmed by the presence of a sperm plug or sperm presence in the vaginal lavage and considered pregnancy or embryonic day (ed) 0. Pregnancy of these "mated" females was confirmed during sonography (see below) on day 10 of pregnancy (ed10) by the presence of fetuses in the uterus. Males were euthanized after pregnancy confirmation in the females. The average number of fetuses/pups per female in this study was 6.1 ± 0.4 (mean ± SEM).

Echocardiography

The females underwent transthoracic two-dimensional echocardiography in order to evaluate maternal LV function at the following time points: non-pregnant diestrous virgin, ed10, pregnancy day 12 (ed12), pregnancy day 18/19 (ed18/19), postpartum day 1.5 (ppd1.5), and postpartum day 7 (ppd7). Some females were sacrificed for tissue collection for RNA isolation on specific days (2 virgin, 2 ed12, 2 ppd1.5, and 8 ppd7 mice), and these mice were used for cardiovascular function correlation with mRNAs with the exception of one ppd7 animal whose tissue was accidentally thawed and had to be discarded. The animals were initially anaesthetized using 4% inhaled isoflurane (Zoetis, Kalamazoo, MI) in oxygen and maintained at 1.5–2% during sonography. Hair was removed from the thoracic region prior to sonography. The VEVO 3100 high-resolution in vivo imaging system (FUJIFILM

VisualSonics, Toronto, ON, Canada) was used to visualize the LV in parasternal short axis view with a 50 MHz transducer generally utilized for adult mouse cardiology. For each animal, measurements used from multiple days all fell within a 20 beat per minute (bpm) range, and the average heart rate of all measurements for all animals was 429 ± 11 bpm (mean ± standard deviation). M-mode imaging of the LV at the midpapillary level was analyzed utilizing VevoLab300 software (FUJIFILM VisualSonics, Toronto, ON, Canada) in order to automatically calculate functional parameters. LV internal diameter during diastole (LVIDd) and systole (LVIDs) and posterior wall thickness during diastole (PWTd) and systole (PWTs) were measured.

Cardiac tissue collection

Animals were euthanized at time points of virgin, ed12, ed18/19, ppd1.5, and ppd7 by cervical dislocation after inhaling isoflurane until the toe pinch reflex was lost. The animal was weighed and then the heart was removed and exsanguinated, rinsed with PBS, and squeezed lightly to remove liquid. The heart was briefly blotted and weighed intact. The LV was then dissected, cut into three pieces, and snap frozen and stored at −80°C until RNA was isolated. For three animals per group, one piece of LV was preserved in paraformaldehyde for later use.

Microarray

We utilized LV RNA from two animals each from diestrous virgin, ed12, ed19, and ppd1.5 mice for pilot microarray analyses to determine highly represented gene pathways that changed during pregnancy. RNA was isolated from one piece of LV tissue using Trizol reagent (Invitrogen, Thermo Fisher Scientific, Waltham, MA) and the RNeasy Mini kit (Qiagen, Germantown, MD). First, Trizol reagent was added to frozen tissue which was then dispersed with 15–20 strokes in a glass dounce homogenizer, and lysates were spun at 12,000*g* at 4°C to clear debris. Subsequent RNA isolation was according to the manufacturer's instructions. RNA samples for microarray analyses were screened for quality by Expirion (Bio-Rad, Hercules, CA) RNA analysis chip. An aliquot of high-quality RNA (n = 2 per group) was sent to the Medical University of South Carolina Proteogenomics Facility for microarray hybridization to Affymetrix GeneChip Mouse Gene 2.0 ST array (Santa Clara, CA). Samples were processed, hybridized, and scanned according to manufacturer protocols. Resulting hybridization data, both the processed image data (CEL files) and RMA normalized hybridization data, were deposited in GEO database (accession GSE114324).

We utilized our microarray dataset and a prior existing microarray dataset from a similar study that compared pregnant and exercised animals, GEO accession GSE36330.[8] The prior study utilized the Affymetrix GeneChip Mouse Genome 430 2.0 array and included samples for diestrous virgin, day 12, day18/19, and ppd0 C57BL/6 mice. Preliminary comparative analyses consistently found that ECM genes were enriched among differentially expressed genes (data not shown), and this group therefore became the focus of further study. For focused analysis of ECM expression data, pairwise comparisons for all groups within each microarray were made using an unadjusted Student's t-test with differential expression criteria set at $P < 0.05$. The mRNAs selected for further study exhibited a difference between at least two animal groups in at least one of the two array datasets. Supplemental Figure 1 shows the heat maps of the ECM pathway genes with significant differences by microarray that were selected for subsequent PCR analyses.

Real-time quantitative PCR

Additional RNA for quantitative PCR (qPCR) was isolated from another piece of LV tissue using Trizol reagent, homogenization as described above and the Direct-zol RNA MiniPrep Plus kit with DNAse I treatment (ZymoResearch, Irvine, CA) in accordance with the manufacturer's protocol. RNA was quantified utilizing a BioPhotometer (Eppendorf) at 260 nm. cDNA was synthesized using the iScript kit (Bio-Rad) and approximately 200 ng of RNA. cDNA was stored at –20°C for usage in qPCR. qPCR was performed using validated mouse primers from Qiagen Superarray (Thermo Fisher), with the exception of *Co11a1* primers. *Col1a1* were forward 5′-GCAATGAAGA ACTGGACTG-3′ and 5′-CTTCTGA GTTGGGTGATACG-3′ were synthesized by Integrated DNA Technologies (Coralville, IA). All PCR primers were initially tested with pooled mouse heart cDNA to confirm single products on melt-curves and were resolved on 2% agarose gels to confirm that amplicons were of the correct size. Individual standard curves were generated from serial dilutions of a known quantity of purified amplicon. The threshold cycle (Ct) values for the target mRNA and the internal control gene ribosomal protein lateral stalk subunit P0 (*Rplp0*) mRNA were used to extrapolate their mRNA quantities from the standard curves. Target mRNA amounts were then normalized to *Rplp0* mRNA amounts. Primer sets utilized in this study included those for the genes tissue inhibitor of metalloproteinase 1, 2, 3, and 4 (*Timp1–4*), matrix metallopeptidase 2, 3, 9, 11, 13, 14, 15, 16, and 28 (*Mmp2*, *3*, *9*, *11*, *13–16*, and *28*), agrin (*Agrn*), collagen, type I, alpha 1 (*Col1a1*), collagen type III, alpha 1 (*Col3a1*), collagen type V, alpha 1 (*Col5a1*), collagen type VIII, alpha 1 (*Col8a1*), fibroblast activation protein (*Fap*), lysyl oxidase (*Lox*), and versican (*Vcan*). We chose to evaluate the expression of *Timp3*, *Mmp9*, *FAP*, and *Lox*, which did not show differential regulation by microarray, because alterations in these ECM mRNAs have been associated with heart pathologies.[21–24] In addition, we wanted to evaluate their gene expression at ppd7, as there was no microarray data for this later time point. PCR was carried out with 4 µl cDNA (equivalent of 5 ng RNA), 1 µl commercial primer mix, and SYBR-green-based Bio-Rad Sso-Advanced Universal Supermix using an I-Cycler (Hercules, CA). The protocol for PCR was as follows: initial denaturation at 95°C for 1 min followed by 35 cycles of denaturation for 15 s at 95°C, annealing 15 s at 60°C, elongation for 30 s at 72°C, then 10 min of final extension at 72°C. For *Col1a1*, the forward and reverse primers were used at 300 nM each and the annealing temperature was 58°C. The melt curve consisted of 80 cycles

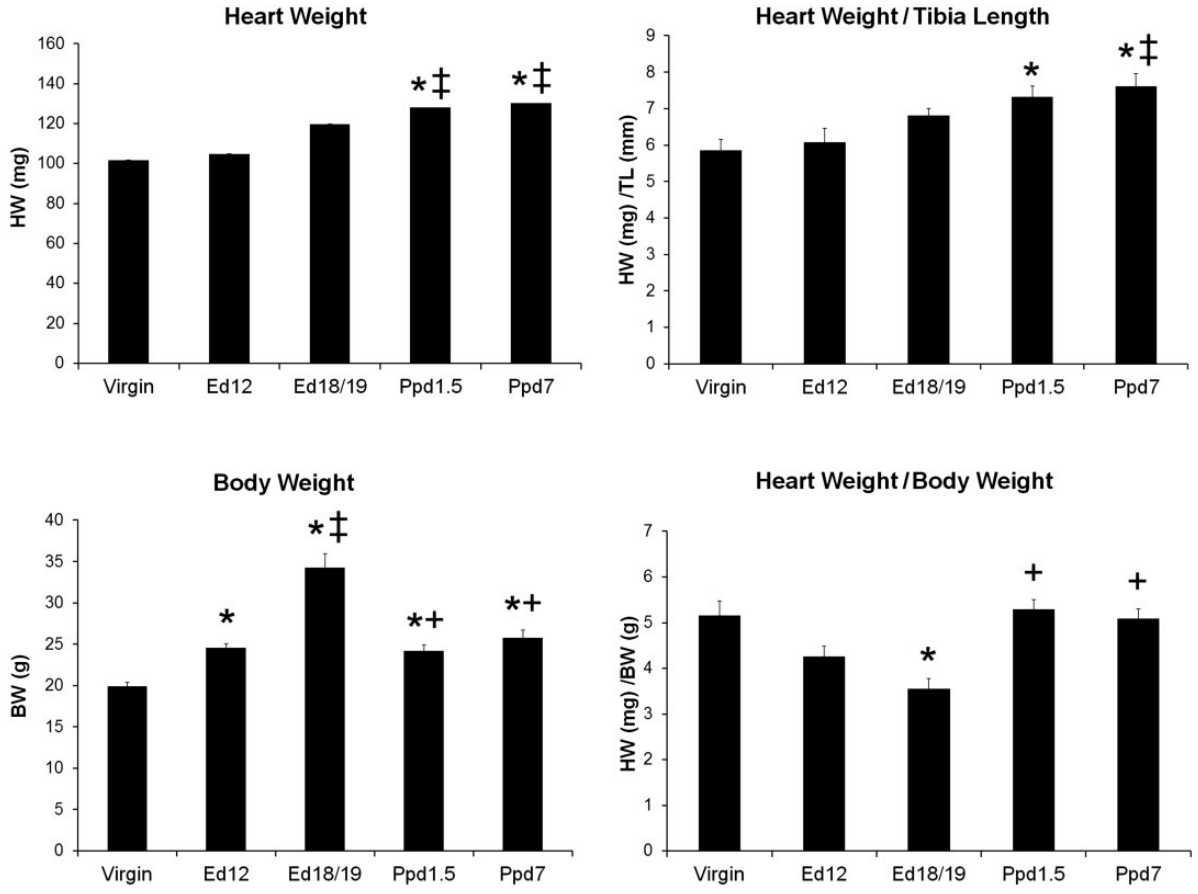

Figure 1. Heart and body weights and heart weight normalized to tibia length and body weight from virgin, pregnant (Ed12 and Ed 18/19), and postpartum mice. Bars indicate means plus SEM. Virgin n = 8, Ed12, Ed18/19 and Ppd1.5 n = 6, and Ppd7 n = 7 animals/group. * indicates significantly different compared with virgin group; ‡ compared with Ed12 group; + compared with Ed18/19 group, $P < 0.05$.
HW: heart weight; TL: tibia length; BW: body weight; Ed: pregnancy or embryonic day; Ppd: postpartum day.

of 0.5°C increments starting at 60°C. Each sample was amplified in at least duplicate wells. A negative control (water) was included for each reaction series.

Data and statistical analysis

Results are presented as the mean ± the standard error of the mean unless specified differently. PCR ratios were ln-transformed for further analyses. All data, including echocardiogram measurements, were then analyzed by ANOVA and followed by Tukey's post-hoc test when ANOVA was significant. Pearson's Correlation coefficients using two-tailed analyses were determined for heart function parameters and LV mRNA levels on the day of sacrifice. Correlation coefficients for all mRNA comparisons with other mRNAs included data from all available animals. Data analyses were performed with GraphPad Prism version 3.02 for Windows (GraphPad Software, Inc., San Diego, CA). $P < 0.05$ was considered statistically significant.

Results

Heart and body weights and ratios

The heart and body weights and heart weight normalized to tibia length (HW/TL) or body weight (HW/BW) at the time of sacrifice for virgin, ed12 and ed18/19 pregnant, and ppd1.5 and ppd7 are shown in Figure 1. Heart weight alone was significantly increased on ppd1.5 and ppd7 compared to virgin and ed12 animals. HW/TL was increased at ppd1.5 and ppd7 compared to virgin mice, and ppd7 was higher than pregnant ed12 mice. Tibia length did not change with reproductive state and was 1.74 ± 0.04 in virgin, 1.73 ± 0.04 in ed12, 1.77 ± 0.04 in ed18/19, 1.75 ± 0.03 in ppd1.5, and 1.71 ± 0.03 cm in ppd7 mice, and thus was used as a non-changing body parameter. Body weight increased with advancing pregnancy and decreased again postpartum, but still remained elevated at both ppd1.5 and ppd7 compared to the virgin group. When heart weight was normalized for body weight, the ratios decreased during late pregnancy (ed18/19) compared to virgin controls and increased again to virgin levels in the postpartum groups.

Echocardiographic assessment

Echocardiography was performed on adult mice in the various reproductive stages stated above with the addition of day 10 of pregnancy to monitor changes in the LV structure and function during pregnancy and in the postpartum period (Figure 2). Neither ejection fraction (EF) nor fractional shortening (FS) was found to be significantly

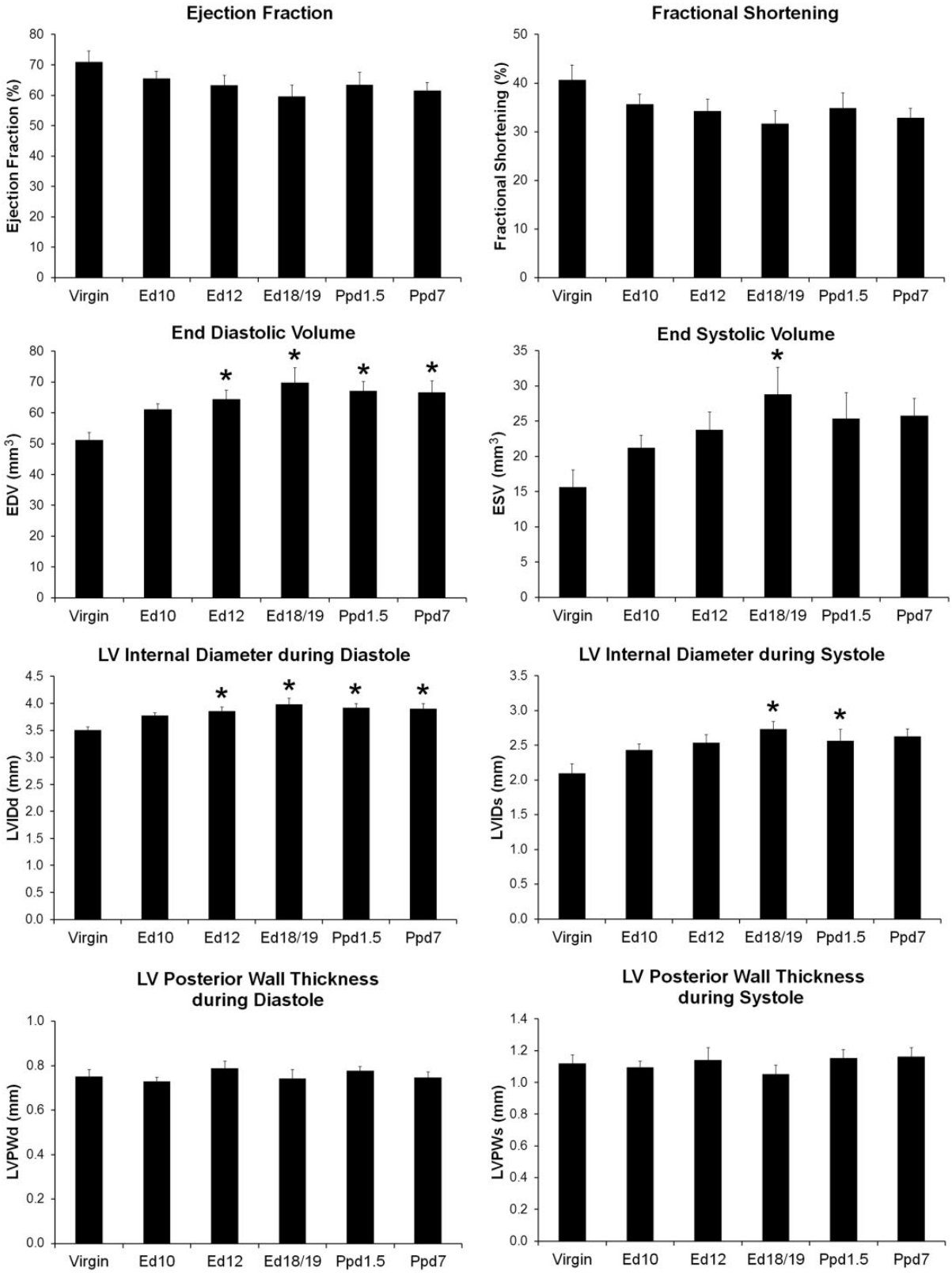

Figure 2. Left ventricle functional parameters from echocardiography in virgin, pregnant (Ed10, Ed12 and Ed 18/19), and postpartum mice. Bars indicate means plus SEM. Virgin n = 12, Ed10 n = 10, Ed12 n = 9, Ed18/19 n = 8, Ppd1.5 n = 10, and Ppd7 n = 8 animals/group. * indicates significantly different compared with virgin group, $P < 0.05$.

EDV: end diastolic volume; ESV: end systolic volume; LVID: left ventricle internal diameter; LV: left ventricle; PWT: posterior wall thickness; Ed: pregnancy or embryonic day; Ppd: postpartum day.

different between groups. LVIDd and end diastolic volume (EDV) were significantly higher than the virgin group at ed12, ed18/19, ppd1.5, and ppd7. LVIDs were higher in ed18/19 and ppd1.5 mice than in virgin mice as was end systolic volume (ESV) at ed18/19. LV posterior wall thickness during both systole and diastole did not differ between groups. Stroke volume (SV = EDV–ESV) was found not to be statistically different between groups (35.6 ± 1.0 virgin, 40.0 ± 1.7 ed10, 40.6 ± 2.5 ed12, 40.0 ± 2.7 ed18/19, 39.8 ± 1.5 ppd1.5, and 40.8 ± 2.5 mm^3 ppd7; n is as in Figure 2 legend).

ECM mRNA levels by reproductive status

The ECM pathway was strongly represented in the referenced microarray analyses and thus specific mRNAs in the gene group were further analyzed by qPCR based on criteria described in the 'Materials and Methods' section. The ECM mRNAs evaluated included *Timp1-4*, *Mmp2*, *3*, *9*, *11*, *13*, *14*, *15*, *16*, *28*, and *Agrn*, *Col1a1 Col3a1*, *Col5a1*, *Col8a1*, *Fap*, *Lox*, and *Vcan*.

The expression profiles of *Timp1-4* mRNAs in LV tissue from female mice at different reproductive states are shown in Figure 3. *Timp1* mRNA levels were more abundant in late pregnancy ed18/19 and early postpartum ppd1.5 mice than in virgin mice, and *Timp1* mRNA in ed18/19 mice was also higher than ed12 mice at midpregnancy. *Timp2* mRNA levels were higher in ed18/19 mice than in ppd7 mice. LV *Timp3* mRNA levels were lower in ppd7 mice compared to the ed12 and ed18/19 pregnant mice. *Timp4* mRNA levels were lower on ppd1.5 compared to virgin, ed12, and ed18/19 mice.

The expression profiles of nine *Mmp* mRNAs in LV tissue from female mice at different reproductive states are shown in Figure 4. For *Mmp3*, mRNA levels of pregnant ed18/19 mice and postpartum day pp1.5 and ppd7 mice were greater than ed12 pregnant mice. *Mmp13* mRNA level was higher in ed18/19 compared to ppd1.5 mice. *Mmp15* mRNA levels were significantly lower in ppd7 mice compared to all other groups. *Mmp2*, *Mmp9*, *Mmp11*, *Mmp14*, *Mmp16*, and *Mmp28* showed no significant differences between groups. Based on the standard curve calculations, *Mmp16* mRNA exhibited the lowest abundance *Mmp* transcripts, and *Mmp15* exhibited the most abundant transcripts.

Quantification of the mRNAs for additional ECM genes is shown in Figure 5. *Col1a1* and *Col3a1* mRNA levels were significantly higher in mouse groups at both ed12 and ed18/19 of pregnancy and both postpartum days compared to virgin mice; there were no other differences between groups for these mRNAs. *Col8a1* mRNA level was higher in both postpartum groups compared ed18/19, and ppd1.5 was higher than ed12. *Agrn*, *Col5a1*, *Fap*, *Lox*, and *Vcan* showed no significant differences between groups.

Using the mice that underwent echocardiography, Pearson correlation coefficients were determined for each

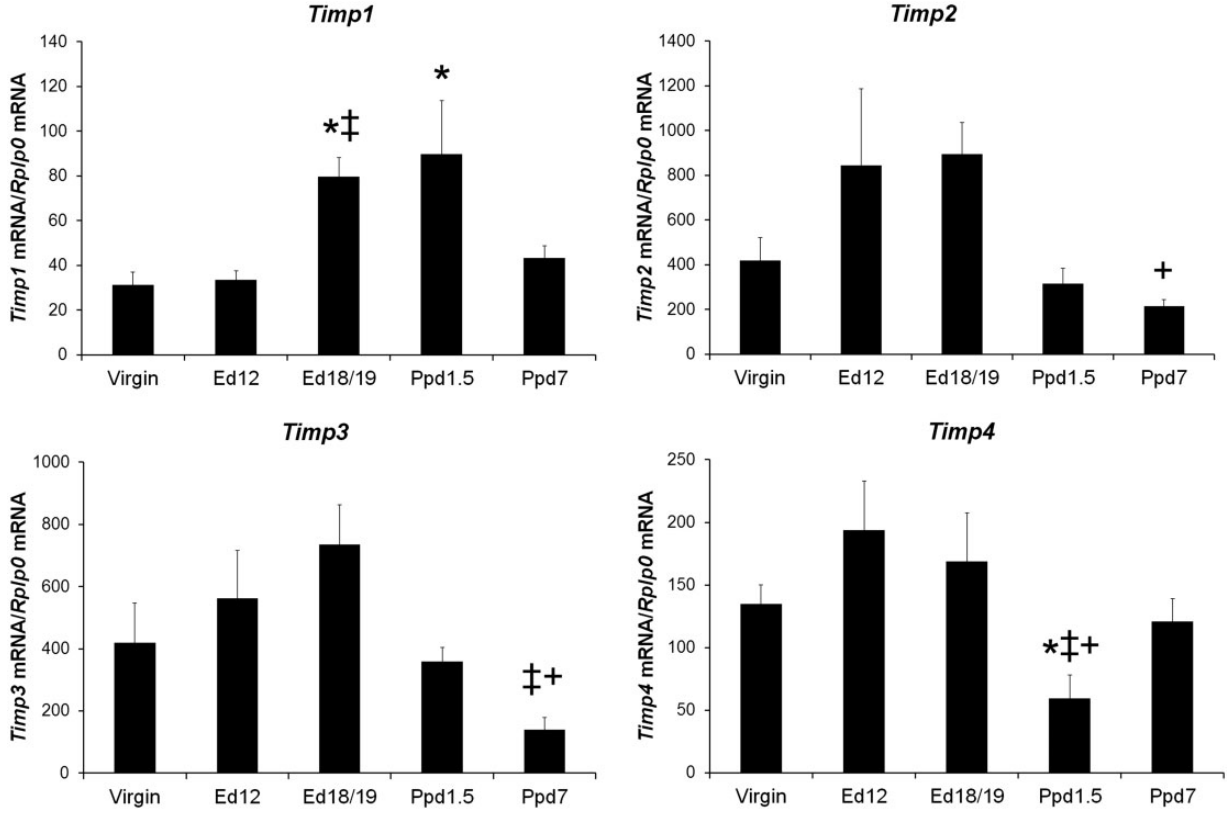

Figure 3. Tissue inhibitor of metalloproteinases mRNA levels in virgin mice and maternal left ventricle tissue. mRNA was reverse transcribed and quantified by real-time PCR using the standard curve method. Target mRNA was normalized for *Rplp0* mRNA. Bars indicate means plus SEM. Virgin n = 8, Ed12, Ed18/19 and Ppd1.5 n = 6, and Ppd7 n = 7 animals/group. * indicates significantly different compared with virgin; ‡ compared with Ed12; + compared with Ed18/19, $P < 0.05$.
Ed: pregnancy or embryonic day; Ppd: postpartum day.

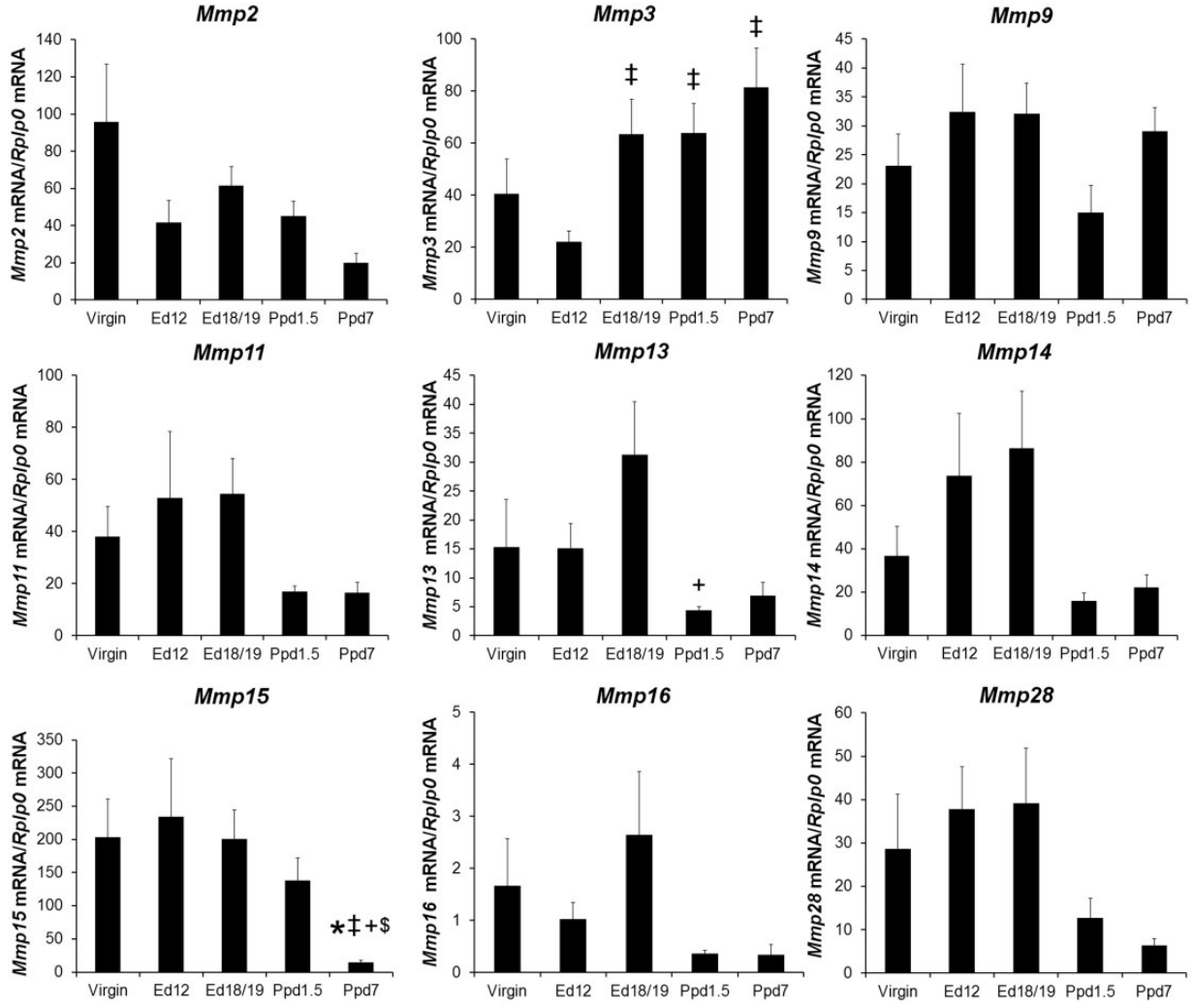

Figure 4. Matrix metalloproteinases mRNA levels in virgin mice and maternal left ventricle tissue. mRNA was quantified as in Figure 3. Bars indicate means plus SEM. Virgin n = 8 animals/group for *Mmps 2*, *9*, *15*, *16*, n = 7 for *Mmps 3*, *11*, *13*, *14*, *28*, Ed12, Ed18/19, and Ppd7 n = 6 animals/group for all mRNAs, Ppd7 n = 7 for *Mmps 2*, *3*, *9*, *11*, *13*, *14*, *15*, *28*, and n = 6 for *Mmp16*. * indicates significantly different compared with virgin; ‡ compared with Ed12; + compared with Ed18; $ compared with Ppd1.5, $P < 0.05$.
Ed: pregnancy or embryonic day; Ppd: postpartum day.

mRNA level and corresponding LV echocardiography measurements on the day of sacrifice (n = 13). Related measurements LVIDd and EDV exhibited correlations of $r = -.57$ and $r = -.58$, respectively, with $P = 0.04$ (for both) with *Timp4*, and $r = .66$ and $r = .67$, respectively, $P = 0.02$ (for both) with *Lox* mRNA levels. LVIDs correlated with *Timp1*, *Timp2*, *MMP14*, and *Lox* mRNAs with $r = .57$, $P = 0.04$, $r = .59$, $P = 0.03$, $r = .61$, $P = 0.03$, and $r = .70$, $P = 0.01$, respectively. Likewise, ESV which derives from LVIDs showed similar correlations with *Timp1*, *Timp2*, *MMP14*, and *Lox* mRNAs with $r = .59$, $P = 0.03$, $r = .62$, $P = 0.02$, $r = .61$, $P = 0.03$, and $r = .71$, $P = 0.01$, respectively. In addition, EF negatively correlated with *Timp1*, *Timp2*, *MMP14*, and *Lox* mRNAs with $r = -.62$, $P = 0.02$, $r = -.70$, $P = 0.01$, $r = -.68$, $P = 0.01$, and $r = -.67$, $P = 0.02$, respectively. Similarly, FS correlated with *Timp1*, *Timp2*, *MMP14*, and *Lox* mRNAs with $r = -.60$, $P = 0.03$, $r = -.67$, $P = 0.01$, $r = -.68$, $P = 0.01$, and $r = -.66$, $P = 0.02$, respectively. LVPWs negatively correlated with *Lox* mRNA levels $r = -.68$, $P = 0.01$. LVPWd and SV showed no significant correlations with mRNA levels.

Correlation analyses were performed to identify coordinated mRNA expressions independent of reproductive status. Table 1 shows the Pearson correlation coefficients for all mRNA level comparisons including all available LV samples (n = 30–33 animals per mRNA). The mRNAs with the fewest interactions (only two each) included *Mmp3* which only correlated with *Timp4* and *Mmp9* mRNA, and *Col1a1* levels which correlated with *Col3a1* and *Co15a1*. The mRNAs with the largest number of significant correlations (13 or 14) were *Mmp11*, *13*, and *14*, followed by (10–11) *Timp2*, *Mmp15*, *16*, and *28*. The strongest correlations (r absolute value $\geq .70$, $P < 0.0001$) included *Timp2* positively with *Timp3*, *Mmp11*, *13*, *15*, *16* and *28*. In addition, *Mmp11* mRNA levels strongly and positively correlated with *Mmp13*, *14*, *16*, and *28*. *Mmp13* mRNA levels had a strong positive correlation with *Mmp14*, *16* and *28*. *Mmp14* also strongly positively correlated with *Mmp16*.

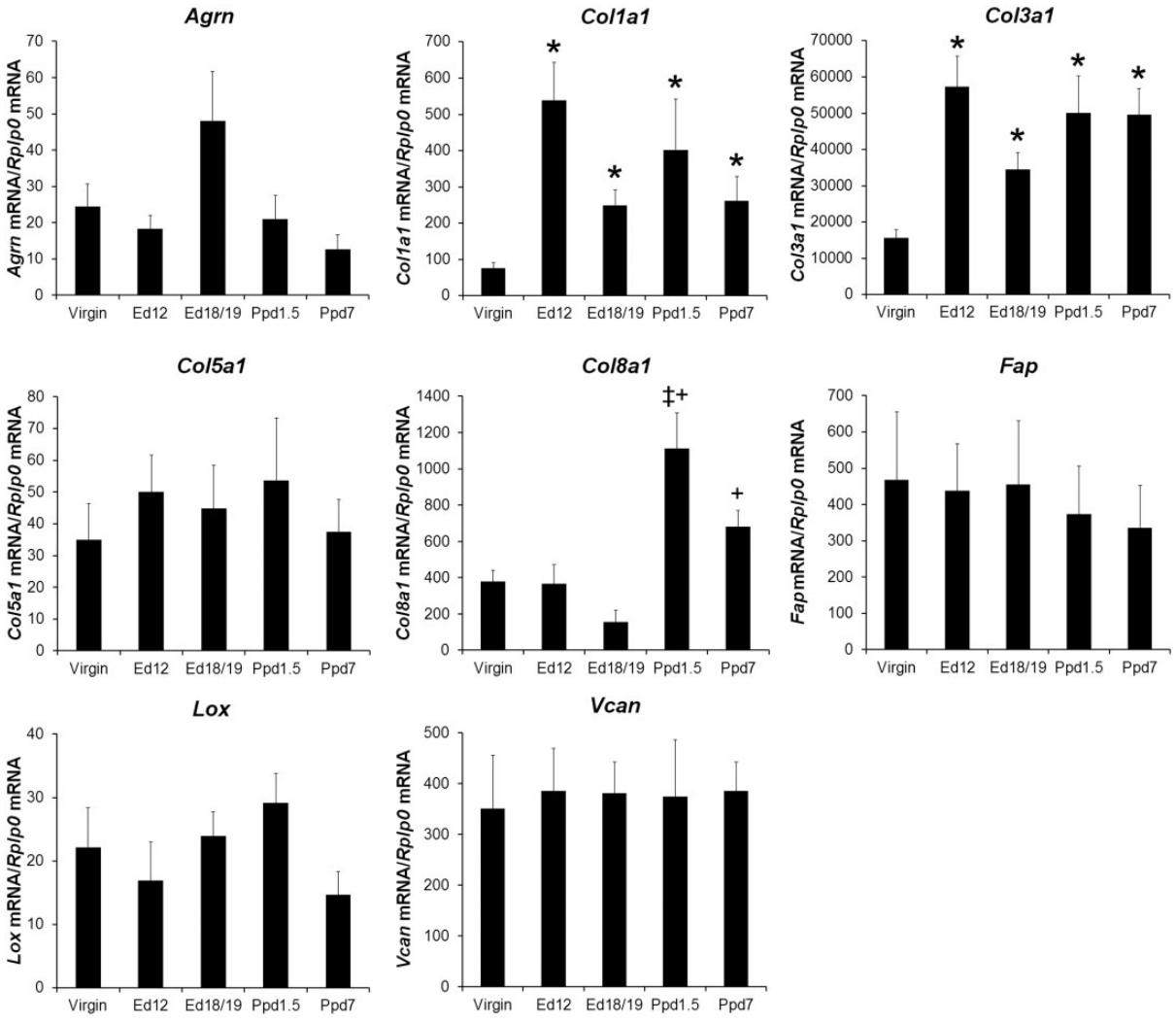

Figure 5. Other selected extracellular matrix proteins mRNA levels in virgin mice and maternal left ventricle tissue. mRNA was quantified as in Figure 3. Bars indicate means plus SEM. Virgin n = 8 animals/group for *Agrn*, *Col8a1*, *Lox*, n = 7 for *Col5a1*, *Fap*, *Vcan*, n = 6 for *Col1a1* and *Col3a1*; Ed12, Ed18/19, and Ppd7 n = 6 animals/group for all mRNAs; Ppd7 n = 7 for *Col3a1*, *Col5a1*, *Col8a1*, *Fap*, and *Vcan*, n = 6 for *Agrn*, *Col1a1*, and *Lox*. * indicates significantly different compared with virgin, ‡ indicates significantly different compared with Ed12; + compared with Ed18 group, $P < 0.05$.
Ed: pregnancy or embryonic day; Ppd: postpartum day.

Mmp16 mRNA exhibited a strong positive correlation with *Mmp28*. Overall, *Col8a1* mRNA exhibited negative correlations ranging from –.38 to –.66 with ten other mRNAs including *Timps 2–4* and *Mmp11, 13–16, 28*, and *Agrn.*

Discussion

Several studies have evaluated heart weight and body weight changes in C57BL/6 mice during pregnancy and at different days postpartum, a few have also measured gene expression changes, and fewer have assessed heart functional parameters. Our study has combined all these endpoints with a focus on ECM gene expression, due to the notable role of ECM proteins in pathological remodeling events.

Previous studies report wet heart weight by itself is increased at late pregnancy or in the postpartum period, and body weight is consistently highest at late pregnancy between 17.5 and 20 days.[5,6,15] Our findings also followed this pattern, although the heart weight was not significantly different in late pregnancy versus non-pregnant animals and was significantly higher in the postpartum period compared to virgin and ed12 pregnant mice. Our studies differ from Umar et al.[6] who reported that HW alone was higher in late pregnancy (day 19/20) compared to virgins and had returned to virgin levels at ppd7. These authors also normalized HW by body weight, and our findings for this ratio are consistent with theirs, in which HW/BW is lower in late pregnancy and similar to non-pregnant animals in the postpartum period. Our findings are most consistent with Ventura et al.[5] who found that wildtype mouse HW/femur length ratios were not significantly different from virgin mice during pregnancy but were heavier during the first two weeks of the postpartum period. Given that body weight increases during pregnancy and decreases postpartum, and that previous studies have shown that tibia and femur length are more stable than body weight and make better normalizers for heart weight, we used

Table 1. Correlation coefficient matrix for extracellular matrix protein mRNAs across all animals.

mRNA	1	2	3	4	5	6	7	8	9	10	11	12	13	14	15	16	17	18	19	20	21
1 *Timp1*	–																				
2 *Timp2*	**.35**	–																			
3 *Timp3*	**.37**	**.77**	–																		
4 *Timp4*	−.24	.27	.17	–																	
5 *Mmp2*	**.37**	**.60**	**.61**	.02	–																
6 *Mmp3*	**.48**	.07	.07	.03	.10	–															
7 *Mmp9*	.16	.23	.10	**.62**	.03	**.43**	–														
8 *Mmp11*	.19	**.80**	**.63**	**.45**	**.60**	.15	**.37**	–													
9 *Mmp13*	.30	**.71**	**.59**	**.37**	**.64**	.17	**.46**	**.80**	–												
10 *Mmp14*	.16	**.64**	**.41**	**.43**	**.38**	.00	**.44**	**.73**	**.76**	–											
11 *Mmp15*	.20	**.76**	**.72**	−.06	**.77**	−.20	−.19	**.62**	**.59**	**.41**	–										
12 *Mmp16*	.22	**.77**	**.62**	.24	**.74**	.03	.27	**.83**	**.83**	**.70**	**.73**	–									
13 *Mmp28*	.16	**.87**	**.70**	.29	**.68**	.10	.21	**.90**	**.75**	**.66**	**.74**	**.82**	–								
14 *Agrn*	.07	**.47**	.34	.26	**.37**	−.09	.24	**.60**	**.41**	**.53**	**.43**	**.53**	**.59**	–							
15 *Col1a1*	.15	.27	.08	.00	.15	−.10	.08	.04	.22	.34	.21	.15	.17	.11	–						
16 *Col3a1*	.09	−.02	−.10	.14	−.13	.21	.25	.03	−.01	.15	−.18	−.14	.04	.14	**.64**	–					
17 *Col5a1*	.08	.13	−.05	**.40**	.20	.01	**.55**	.35	.33	**.58**	−.01	0.29	.22	**.45**	**.43**	**.56**	–				
18 *Col8a1*	.09	**−.66**	**−.38**	**−.47**	−.17	.10	−.31	**−.62**	**−.61**	**−.63**	**−.44**	**−.53**	**−.59**	**−.40**	−.07	.10	−.13	–			
19 *Fap*	−.01	.24	.15	.25	.30	.10	.29	**.47**	**.40**	**.44**	.25	**.37**	**.41**	**.53**	.06	**.38**	**.53**	−.25	–		
20 *Lox*	**.41**	.11	.33	−.33	**.68**	.26	−.11	.09	.34	−.01	**.42**	.33	.24	.08	.14	.01	−.01	.29	.22	–	
21 *Vcan*	.11	.09	.10	.28	.08	.19	**.60**	.24	**.36**	**.40**	−.08	.23	.23	.33	.19	**.45**	**.65**	−.12	**.60**	.13	–

Note: Bold font indicates significant correlation between the two mRNAs, $P < 0.05$. n = 30–33 animals per comparison.

HW/TL ratios to normalize changes in heart weight during pregnancy.[25] Slight differences between studies may also be due to how much blood remains in the heart wall when weighed and a better comparison would be dry heart weights.

Pregnancy is known to cause a reversible physiological eccentric hypertrophy of the heart.[4] LV echocardiographic measurements give structural and functional information about the heart. Although we did not see a significant change in LV EF and FS with reproductive status in our study, EF and FS are calculated from LVIDd and LVIDs,[26] and these measurements were higher during pregnancy and at one (LVIDs) or both days (LVIDd) postpartum period compared to virgin mice. Eghbali et al.[9] compared mice at diestrus and late pregnancy (day 19/20) and found reduced LV EF and FS when comparing just the two groups. Furthermore, concordant with our study, LV internal diameters were also increased in late pregnant mice compared to non-pregnant virgin mice in the Eghbali study. In a similar study, Umar et al.[6] reported EF was mildly decreased at late pregnancy and restored by ppd1 when compared to virgin animals. In our study, ESV was no longer significantly elevated at ppd1.5 and ppd7, and LVIDs was no longer elevated at ppd7, whereas the diastolic EDV and LVIDd parameters remained elevated postpartum. These findings suggest that systolic LV function normalizes in postpartum animals before diastolic function does. Although there are discrepancies about the exact day for significant cardiac functional changes in mice, the changes are consistently significant in the peripartum period and consistently reflect the enlargement of the LV chamber.

ECM is maintained by a balance of protein breakdown and new synthesis, a process commonly known as ECM remodeling. TIMPs and MMPs play a major part in this process.[27] We chose to focus on TIMPs and MMPs partly because of their previously demonstrated mRNA and protein alterations during cardiac remodeling under pathological conditions.[19] TIMPs are known for their wide ability to inhibit multiple metalloproteinase activities, although their effectiveness can vary by target.[28] For example, TIMP1 is less effective at inhibiting membrane-type MMPs including MMP14, 15, and 16, while both TIMP1 and TIMP3 interact with MMP9. The relationship between some TIMPs and MMPs is complex, such as with TIMP2, MMP2 and MMP14. MMP14 is needed for pro-MMP2 activation.[29] TIMP2 inhibits MMP14 activity but also associates with pro-MMP2, which can then be activated by adjacent active MMP14 molecules. TIMP4 can also inhibit MMP14 but does not recruit pro-MMP2. The molecular ratio between TIMPs and MMPs also contributes to ECM turnover.[30] TIMPs, especially TIMP3, can also inhibit other proteases in the ADAMS and ADAMTS families.[28]

In our study, with the exception of *Timp1* mRNA, which was significantly increased at ppd1.5, *Timp2–4* tended to be lowest at one or both time points in the postpartum period. Despite this pattern associated with pregnancy status, only *Timp2* and *Timp3* mRNA levels highly correlated with each other. Interestingly, *Timp4* mRNA levels were lowest at ppd1.5 and recovered to virgin levels by ppd7; this suggests that particular TIMP4 targets might experience less inhibition immediately postpartum. If protein and activity levels parallel mRNA levels, then it is possible that TIMP1 acts on targets such as MMP3 which was the only *Mmp* mRNA to be increased in the postpartum period. Our finding that *Timp1* mRNA at ppd1.5 was higher than virgin mice is consistent with the study of Chung et al.[7] that found *Timp1* mRNA was significantly increased at ppd0 compared to non-pregnant mice. Interestingly, in our study, *Timp1* and *Timp2* mRNA correlated with heart

parameters ESV, LVIDs, EF and FS, and *Timp4* mRNA correlated with EDV and LVIDd, providing a possible link of their proteins to heart function.

TIMP1 is increased in profibrotic pathologic cardiac conditions.[28] Deletion of *Timp1* in mice led to decreased myocardial fibrillar collagen content and increased LV wall stress.[31] In addition, TIMP1 overexpression in embryonic stem cells was found to protect the heart in an infarcted mouse model and reduced myocyte apoptosis.[32] The elevated *Timp1* mRNA we observed at day 1.5 postpartum may increase TIMP1 protein levels which could inhibit MMPs or other proteases during the peripartum period allowing for a gradual return to baseline LV structure and function postpartum.

MMPs include collagenases, gelatinases, stromelysins, and proteases which degrade numerous ECM proteins.[30] Their actions not only lead to ECM turnover but can facilitate growth factor release from the matrix, activation of other MMPs, cell migration and proliferation, and cell survival. Of the 28 known MMPs, we examined the mRNAs for *Mmp2*, *3*, *9*, *11*, *13*, *14*, *15*, *16*, and *28*. Their corresponding proteins have a number of overlapping activities with several targeting many of the same collagens, gelatin, elastin, fibronectin, laminins, versican, entactin, and other ECM constituents. Many MMP substrates overlap; yet, their mechanisms of activation differ. For example, MMP2 is activated by MMP14, and MMP3 is activated by various proteinases including trypsin and plasmin.[33]

Umar et al. evaluated *Mmp2* mRNA in LV from non-pregnant, late pregnant (ed 19/20), and ppd7 mice ($n = 4$ animals/day, by ANOVA and Bonferroni test).[6] In their study, *Mmp2* mRNA was lower in late pregnancy than virgin animals and partially recovered to virgin levels on ppd7. Our findings vary in that a change in *Mmp2* mRNA did not occur with pregnancy status. As these studies also utilized C57BL/6 mice of approximately the same age, the different findings may be due to different animal numbers per group, litter size, statistical methods employed, animal vendors, and/or housing environments. Chung et al.[7] found *Mmp3* mRNA higher during late pregnancy and ppd0 higher than non-pregnant animals ($n = 6$ animals/day, using multiple t-tests), we observed similar late pregnancy and early postpartum *Mmp3* elevation, and also found it higher at ppd7.

Mmp11, *13*, *14*, *16*, and *28* had a similar expression profiles with their mRNA expressions positively correlated with each other suggesting the possibility of coordinated regulation within animals irrespective of pregnancy status. However, out of the *Mmp* mRNAs, only *Mmp13* and *Mmp15* mRNA achieved significant decreases postpartum. This may be due in part to the greater variability we observed in *Mmp* mRNA expressions in virgin and pregnant mice than postpartum mice. Interestingly, *Mmp14* was the only *Mmp* mRNA to correlate with any heart function measurement and these parameters were all associated with systolic function (EF, FS, ESV, and LVIDs).

Estrogen and progesterone levels change during pregnancy and during the postpartum period which could potentially regulate the measured gene changes in peripartum and postpartum mice. For example, several MMPs have been reported to be regulated by estrogen and/or progesterone, but the pattern of regulation varies by cellular setting.[34] Cardiac MMP2 and MMP9 expression and activity during volume overload in non-pregnant female rats is decreased by estrogen,[35] whereas in vascular smooth muscle cells estrogen increases active MMP2.[36] MMP2 and MMP9 levels and activity in the rat uterus and aorta are increased during pregnancy, an effect which is recapitulated by estrogen plus progesterone treatment of virgin animals.[37] In mice, plasma estradiol and progesterone increase with advancing pregnancy, progesterone levels fall just before parturition, and there is a small transient increase in estradiol during the peripartum window.[38,39] Estradiol levels then fall off during lactation, and progesterone levels are low in the first week of lactation.[40] The lower levels of specific *Timp* and *Mmp* mRNAs in the postpartum period may reflect the low level of sex steroid hormones during this period. A more detailed analysis of estrogen and progesterone effects on cardiac ECM during pregnancy is warranted based on our current findings.

In addition to the *Timp* and *Mmp* genes, eight other mRNAs encoding ECM proteins with diverse functions were evaluated for expression differences during pregnancy and the postpartum period. Four genes encoding collagens with different functions were investigated. *Col1a1* and *Col3a1*, which encode chains of the major heart fibrillar collagens type I and type III,[41] increased with pregnancy and stayed elevated postpartum. A study in rats also found the genes for collagen type I and III elevated in pregnancy, but only increased collagen type III protein.[42] Analysis of collagen I/III content using Sirius red staining of heart tissue in rats has shown no net increase in collagen content during pregnancy,[43] and fibrosis during pregnancy is minimal or absent.[4] If the collagen I and/or collagen III protein are made, they are likely being turned over rapidly or redistributed. A further analysis of the distribution of the collagen I and III proteins in heart tissue is needed to determine this. *Col8a1* mRNA showed upregulation in the postpartum period compared to pregnancy, whereas *Col5a1* mRNA was not regulated. This finding suggests that collagen type VIII protein could be increased in the postpartum period as well. Collagen type VIII is a non-fibrillar short chain collagen made from the products of the *Col8a1* and *Col8a2* genes, and in the heart is made by endothelial cells and cardiac fibroblasts.[44,45] Deletion of the *Col8a1/2* genes in mice followed by induced pressure overload of the heart showed reduced fibrosis but increased dilatation and mortality compared to wildtype controls.[45] These and other studies indicate collagen type VIII contributes to heart wall and blood vessel wall integrity.[46] Collagen type V is a fibrillar collagen made by protein products of either the *Col5a1* gene alone or in combination with proteins encoded by the *Col5a2* and *Col5a3* genes. Collagen type V helps to organize type I collagen and makes contact with basement membranes.[47]

Agrn and *Vcan* mRNAs encode two different proteoglycans and showed no regulation with pregnancy or postpartum. Agrin encoded by the *Agrn* gene forms a heparin sulfate proteoglycan associated with neuromuscular

junction structure.[48] Recently, agrin was identified as an ECM component needed for cardiac myocyte regeneration in the neonatal heart and is reduced with age and the loss of myocyte regenerative capacity.[49] Versican, a hygroscopic chondroitin sulfate proteoglycan, derives from the *Vcan* gene and has been shown to play a role in heart development and angiogenesis.[50] It binds hyaluronin and contributes to ECM assembly.

Expression level of the mRNAs for two diverse extracellular matrix enzymes, fibroblast activation protein alpha (FAP) and lysyl oxidase (LOX) were also quantified and found not to be regulated. FAP is a fibroblast-derived protease not belonging to the MMP family.[51] It has the ability to cleave collagen and gelatin. FAP was elevated in the border zone of cardiac infarcts in rats, and thus increased levels are thought to be associated with areas of intense remodeling.[23] *Lox* encodes one of several members of the lysyl oxidase family. In the ECM, lysyl oxidase is responsible for cross-linking collagen and elastin giving it stability and tensile strength contributing to mechanical properties of the LV.[52,53] Although *Lox* mRNA did not vary with reproductive state, it correlated with almost all heart functional parameters measured including EDV, ESV, LVIDd, LVIDs, FS, EF, and LVPWs.

In summary, of the non-*Timp* and non-*Mmp* family ECM genes evaluated only three collagen genes *Col1a1*, *Col3a1*, and *Col8a1* mRNA showed significant changes, indicating that gene changes observed in this study are specific to certain ECM molecules and are not universal to proteins within the ECM. A corresponding increase in collagen type VIII protein would contribute to new matrix formation in the postpartum remodeling period especially in the subendothelial regions or vessel walls.

Pregnancy creates a type of volume overload on the heart that is similar in some respects to pathological volume overload phenotypes.[54] With both conditions, there is an increase in myocyte length that allows for enlargement of the LV chamber.[19] Rodent models of chronic cardiac volume overload show an initial phase of no mortality, a compensated phase with increased mortality prior to a decompensated phase where signs of heart failure are evident.[22] Such models differ from pregnancy in that pregnancy has a slower increase in the volume overload seen by the heart, and the volume overload condition resolves over time in the postpartum period. The rodent aortocaval fistula volume overload model exhibits increased Mmp activity in the first couple of weeks and increases in gene expression for collagen types I and III, and ultimately altered ratios of these collagens, changes in Timp1/2 and Mmp2/9 abundance and/or activity.[22,32] Ultimately, pathological volume overload models exhibit increased fibrosis, a condition not seen with normal pregnancy.[4]

One of the limitations of our study is that we only examined mRNA expression changes and have not looked at protein abundances or activities due to limited LV tissue availability per mouse. Based on our findings of our study, we plan to do future work utilizing more animals to assess the levels and activities of proteins encoded by those mRNAs showing significant differences. In addition, a better assessment of the relationship between mRNA levels and heart function measurements will need a larger analysis with more animals of different reproductive states as our correlations were based on 13 animals. Our study also found that some of the mRNAs that we selected from microarray data were not regulated when evaluated by qPCR. This could be for several reasons. First, we utilized t-tests to identify potential differences between groups because few genes reached a two-fold difference by microarray. In addition, the number of animals used for each microarray time point was two or three, whereas our qPCR analyzed six to eight animals per time point. Moreover, oligonucleotide microarrays are less specific and can potentially hybridize with highly similar cDNAs, while qPCR is designed for single products. In addition, small fold-changes with microarray are found to be less reliable.[55] Despite these limitations, our study has yielded new data regarding pregnancy and the postpartum period ECM gene changes upon which to build. Our new findings show regulation of all *Timp*, add *Mmp13* and *Mmp15* to known regulation of *Mmp3*, and show the patterns of *Col1a1*, *Col3a1*, and *Col8a1* mRNAs in mouse during pregnancy and the postpartum period. In addition, we have made a comprehensive echocardiographic analyses of mouse heart functional parameters at multiple days of pregnancy and postpartum which has not been previously reported. Finally, we used correlation analyses to assess the coordinated profiles of different mRNAs with each other independent of reproductive status, and also found specific mRNAs to correlate with echocardiographic measurements. Using this information, we plan to examine specific *Timp* and *Mmp* gene overexpression and knockout mouse models that have cardiac phenotypes to better understand critical changes in ECM that may give rise to postpartum cardiomyopathy.

Authors' contributions: HAL designed the experiments. JLB performed the microarray data analyses. EA, DLB, RNM, MP, and HAL conducted the experiments and collected data. MEP and HAL analyzed the data and wrote the article. All authors participated in editing the article.

ACKNOWLEDGMENTS

We thank Dr. Edie Goldsmith for mouse *Col1a1* primers and helpful discussions, Charity Fix for assistance with tibia measurements, and Dr. Ambrish Kumar for echocardiography assistance.

DECLARATION OF CONFLICTING INTERESTS

The author(s) have no potential conflicts of interest with respect to the research, authorship, and/or publication of this article.

FUNDING

The author(s) disclosed receipt of the following financial support for the research, authorship, and/or publication of this article: Work from Medical University of SC Proteogenomics Facility was supported by NIH grants P30GM103342 and P20GM103499 and Medical University of SC's Office of the

Vice President for Research. Work at the University of South Carolina was supported by an INBRE pilot project and DRP award to HL also funded by 5P20GM103499.

ORCID iD

Holly A LaVoie http://orcid.org/0000-0002-6658-549X

REFERENCES

1. de Haas S, Ghossein-Doha C, van Kuijk SM, van Drongelen J, Spaanderman ME. Physiological adaptation of maternal plasma volume during pregnancy: a systematic review and meta-analysis. *Ultrasound Obstet Gynecol* 2017;**49**:177–87
2. Schannwell CM, Schneppenheim M, Plehn G, Marx R, Strauer BE. Left ventricular diastolic function in physiologic and pathologic hypertrophy. *Am J Hypertens* 2002;**15**:513–7
3. Hunyor SN. Vascular, volume, and cardiac response to normal and hypertensive pregnancy. *Hypertension* 1984;**6**:129–32
4. Li J, Umar S, Amjedi M, Iorga A, Sharma S, Nadadur RD, Regitz-Zagrosek V, Eghbali M. New frontiers in heart hypertrophy during pregnancy. *Am J Cardiovasc Dis* 2012;**2**:192–207
5. Ventura NM, Li TY, Tse MY, Andrew RD, Tayade C, Jin AY, Pang SC. Onset and regression of pregnancy-induced cardiac alterations in gestationally hypertensive mice: the role of the natriuretic peptide system. *Biol Reprod* 2015;**93**:142
6. Umar S, Nadadur R, Iorga A, Amjedi M, Matori H, Eghbali M. Cardiac structural and hemodynamic changes associated with physiological heart hypertrophy of pregnancy are reversed postpartum. *J Appl Physiol (1985)* 2012;**113**:1253–9
7. Chung E, Heimiller J, Leinwand LA. Distinct cardiac transcriptional profiles defining pregnancy and exercise. *PLoS One* 2012;**7**:e42297
8. Eghbali M, Wang Y, Toro L, Stefani E. Heart hypertrophy during pregnancy: a better functioning heart? *Trends Cardiovasc Med* 2006;**16**:28591
9. Eghbali M, Deva R, Alioua A, Minosyan TY, Ruan H, Wang Y, Toro L, Stefani E. Molecular and functional signature of heart hypertrophy during pregnancy. *Circ Res* 2005;**96**:1208–16
10. Jankowski M, Wang D, Mukaddam-Daher S, Gutkowska J. Pregnancy alters nitric oxide synthase and natriuretic peptide systems in the rat left ventricle. *J Endocrinol* 2005;**184**:209–17
11. Weiner CP, Knowles RG, Moncada S. Induction of nitric oxide synthases early in pregnancy. *Am J Obstet Gynecol* 1994;**171**:838–43
12. Redondo-Angulo I, Mas-Stachurska A, Sitges M, Giralt M, Villarroya F, Planavila A. C/EBPbeta is required in pregnancy-induced cardiac hypertrophy. *Int J Cardiol* 2016;**202**:819–28
13. Redondo-Angulo I, Mas-Stachurska A, Sitges M, Tinahones FJ, Giralt M, Villarroya F, Planavila A. Fgf21 is required for cardiac remodeling in pregnancy. *Cardiovasc Res* 2017;**113**:1574–84
14. Chung E, Yeung F, Leinwand LA. Calcineurin activity is required for cardiac remodelling in pregnancy. *Cardiovasc Res* 2013;**100**:402–10
15. Iorga A, Dewey S, Partow-Navid R, Gomes AV, Eghbali M. Pregnancy is associated with decreased cardiac proteasome activity and oxidative stress in mice. *PLoS One* 2012;**7**:e48601
16. Gonzalez AM, Osorio JC, Manlhiot C, Gruber D, Homma S, Mital S. Hypertrophy signaling during peripartum cardiac remodeling. *Am J Physiol Heart Circ Physiol* 2007;**293**:H3008–13
17. Aasa KL, Zavan B, Luna RL, Wong PG, Ventura NM, Tse MY, Carmeliet P, Adams MA, Pang SC, Croy BA. Placental growth factor influences maternal cardiovascular adaptation to pregnancy in mice. *Biol Reprod* 2015;**92**:44
18. Carmos-Silva C, Almeida JF, Macedo LM, Melo MB, Pedrino GR, Santos FF, Biancardi MF, Santos RA, Carvalho AA, Mendes EP, Colugnati DB, Mazaro-Costa R, Castro CH. Mas receptor contributes to pregnancy-induced cardiac remodeling. *Clin Sci (Lond)* 2016;**130**:2305–16
19. Spinale FG. Myocardial matrix remodeling and the matrix metalloproteinases: influence on cardiac form and function. *Physiol Rev* 2007;**87**:1285–342
20. Goldman JM, Murr AS, Cooper RL. The rodent estrous cycle: characterization of vaginal cytology and its utility in toxicological studies. *Birth Defect Res B* 2007;**80**:84–97
21. El Hajj EC, El Hajj MC, Ninh VK, Gardner JD. Inhibitor of lysyl oxidase improves cardiac function and the collagen/MMP profile in response to volume overload. *Am J Physiol Heart Circ Physiol* 2018;**315**:H463–H73
22. Janicki JS, Brower GL, Gardner JD, Forman MF, Stewart JA Jr, Murray DB, Chancey AL. Cardiac mast cell regulation of matrix metalloproteinase-related ventricular remodeling in chronic pressure or volume overload. *Cardiovasc Res* 2006;**69**:657–65
23. Tillmanns J, Hoffmann D, Habbaba Y, Schmitto JD, Sedding D, Fraccarollo D, Galuppo P, Bauersachs J. Fibroblast activation protein alpha expression identifies activated fibroblasts after myocardial infarction. *J Mol Cell Cardiol* 2015;**87**:194–203
24. Kandalam V, Basu R, Abraham T, Wang X, Awad A, Wang W, Lopaschuk GD, Maeda N, Oudit GY, Kassiri Z. Early activation of matrix metalloproteinases underlies the exacerbated systolic and diastolic dysfunction in mice lacking TIMP3 following myocardial infarction. *Am J Physiol Heart Circ Physiol* 2010;**299**:H1012–23
25. Yin FC, Spurgeon HA, Rakusan K, Weisfeldt ML, Lakatta EG. Use of tibial length to quantify cardiac hypertrophy: application in the aging rat. *Am J Physiol* 1982;**243**:H941–7
26. Gao S, Ho D, Vatner DE, Vatner SF. Echocardiography in mice. *Curr Protoc Mouse Biol* 2011;**1**:71–83
27. Louzao-Martinez L, Vink A, Harakalova M, Asselbergs FW, Verhaar MC, Cheng C. Characteristic adaptations of the extracellular matrix in dilated cardiomyopathy. *Int J Cardiol* 2016;**220**:634–46
28. Arpino V, Brock M, Gill SE. The role of TIMPs in regulation of extracellular matrix proteolysis. *Matrix Biol* 2015;**44–46**:247–54
29. Hernandez-Barrantes S, Bernardo M, Toth M, Fridman R. Regulation of membrane type-matrix metalloproteinases. *Semin Cancer Biol* 2002;**12**:131–8
30. Liu J, Khalil RA. Matrix metalloproteinase inhibitors as investigational and therapeutic tools in unrestrained tissue remodeling and pathological disorders. *Prog Mol Biol Transl Sci* 2017;**148**:355–420
31. Roten L, Nemoto S, Simsic J, Coker ML, Rao V, Baicu S, Defreyte G, Soloway PJ, Zile MR, Spinale FG. Effects of gene deletion of the tissue inhibitor of the matrix metalloproteinase-type 1 (TIMP-1) on left ventricular geometry and function in mice. *J Mol Cell Cardiol* 2000;**32**:109–20
32. Glass C, Singla DK. Overexpression of TIMP-1 in embryonic stem cells attenuates adverse cardiac remodeling following myocardial infarction. *Cell Transplant* 2012;**21**:1931–44
33. Visse R, Nagase H. Matrix metalloproteinases and tissue inhibitors of metalloproteinases: structure, function, and biochemistry. *Circ Res* 2003;**92**:827–39
34. Chen J, Khalil RA. Matrix metalloproteinases in normal pregnancy and preeclampsia. *Prog Mol Biol Transl Sci* 2017;**148**:87–165
35. Voloshenyuk TG, Gardner JD. Estrogen improves TIMP-MMP balance and collagen distribution in volume-overloaded hearts of ovariectomized females. *Am J Physiol Regul Integr Comp Physiol* 2010;**299**:R683–93
36. Mountain DJ, Kirkpatrick SS, Freeman MB, Stevens SL, Goldman MH, Grandas OH. Role of MT1-MMP in estrogen-mediated cellular processes of intimal hyperplasia. *J Surg Res* 2012;**173**:224–31
37. Dang Y, Li W, Tran V, Khalil RA. EMMPRIN-mediated induction of uterine and vascular matrix metalloproteinases during pregnancy and in response to estrogen and progesterone. *Biochem Pharmacol* 2013;**86**:734–47
38. Barkley MS, Geschwind II, Bradford GE. The gestational pattern of estradiol, testosterone and progesterone secretion in selected strains of mice. *Biol Reprod* 1979;**20**:733–8
39. Chung E, Yeung F, Leinwand LA. Akt and MAPK signaling mediate pregnancy-induced cardiac adaptation. *J Appl Physiol (1985)* 2012;**112**:1564–75
40. deCatanzaro D, Muir C, Beaton EA, Jetha M. Non-invasive repeated measurement of urinary progesterone, 17beta-estradiol, and testosterone in developing, cycling, pregnant, and postpartum female mice. *Steroids* 2004;**69**:687–96
41. de Souza RR. Aging of myocardial collagen. *Biogerontology* 2002;**3**:325–35

42. Limon-Miranda S, Salazar-Enriquez DG, Muniz J, Ramirez-Archila MV, Sanchez-Pastor EA, Andrade F, Sonanez-Organis JG, Moran-Palacio EF, Virgen-Ortiz A. Pregnancy differentially regulates the collagens types I and III in left ventricle from rat heart. *Biomed Res Int* 2014;**2014**:984785
43. Aljabri MB, Songstad NT, Lund T, Serrano MC, Andreasen TV, Al-Saad S, Lindal S, Sitras V, Acharya G, Ytrehus K. Pregnancy protects against antiangiogenic and fibrogenic effects of angiotensin II in rat hearts. *Acta Physiol (Oxf)* 2011;**201**:445–56
44. Shuttleworth CA. Type VIII collagen. *Int J Biochem Cell Biol* 1997;**29**:1145–8
45. Skrbic B, Engebretsen KV, Strand ME, Lunde IG, Herum KM, Marstein HS, Sjaastad I, Lunde PK, Carlson CR, Christensen G, Bjornstad JL, Tonnessen T. Lack of collagen VIII reduces fibrosis and promotes early mortality and cardiac dilatation in pressure overload in mice. *Cardiovasc Res* 2015;**106**:32–42
46. Sinha S, Kielty CM, Heagerty AM, Canfield AE, Shuttleworth CA. Upregulation of collagen VIII following porcine coronary artery angioplasty is related to smooth muscle cell migration not angiogenesis. *Int J Exp Pathol* 2001;**82**:295–302
47. Mak KM, Png CY, Lee DJ. Type V collagen in health, disease, and fibrosis. *Anat Rec (Hoboken)* 2016;**299**:613–29
48. Bezakova G, Ruegg MA. New insights into the roles of agrin. *Nat Rev Mol Cell Biol* 2003;**4**:295
49. Bassat E, Mutlak YE, Genzelinakh A, Shadrin IY, Baruch Umansky K, Yifa O, Kain D, Rajchman D, Leach J, Riabov Bassat D, Udi Y, Sarig R, Sagi I, Martin JF, Bursac N, Cohen S, Tzahor E. The extracellular matrix protein agrin promotes heart regeneration in mice. *Nature* 2017;**547**:179–84
50. Sotoodehnejadnematalahi F, Burke B. Structure, function and regulation of versican: the most abundant type of proteoglycan in the extracellular matrix. *Acta Med Iran* 2013;**51**:740–50
51. Park JE, Lenter MC, Zimmermann RN, Garin-Chesa P, Old LJ, Rettig WJ. Fibroblast activation protein, a dual specificity serine protease expressed in reactive human tumor stromal fibroblasts. *J Biol Chem* 1999;**274**:36505–12
52. Kumari S, Panda TK, Pradhan T. Lysyl oxidase: its diversity in health and diseases. *Indian J Clin Biochem* 2017;**32**:134–41
53. Lopez B, Gonzalez A, Hermida N, Valencia F, de Teresa E, Diez J. Role of lysyl oxidase in myocardial fibrosis: from basic science to clinical aspects. *Am J Physiol Heart Circ Physiol* 2010;**299**:H1–9
54. Bollen IA, Van Deel ED, Kuster DW, Van Der Velden J. Peripartum cardiomyopathy and dilated cardiomyopathy: different at heart. *Front Physiol* 2014;**5**:531.
55. Morey JS, Ryan JC, Van Dolah FM. Microarray validation: factors influencing correlation between oligonucleotide microarrays and real-time PCR. *Biol Proced Online* 2006;**8**:175–93

(Received June 18, 2018, Accepted November 20, 2018)